CrystEngComm

Accepted Manuscript

ROYAL SOCIETY OF CHEMISTRY

www.rsc.org/crystengcomm

Sandwich Crystals of Butyl Paraben

Huaiyu Yang[a,b] *Hong Chen*[c,d] *and Åke C Rasmuson*[a,e]*

a) KTH Royal Institute of Technology, Department of Chemical Engineering and Technology, Stockholm, Sweden

b) Solid-State Research Group, Strathclyde Institute of Pharmacy and Biomedical Sciences, University of Strathclyde, Glasgow

c) Stockholm University, Department of Materials and Environmental Chemistry, Stockholm, Sweden

d) China University of Geosciences, Department of Material Science and Chemistry, Wuhan, P.R. China

e) University of Limerick, Department of Chemical and Environmental Science, Solid State Pharmaceutical Cluster, Materials and Surface Science Institute, Limerick, Ireland

*Corresponding author: Åke C Rasmuson; Telephone: *+46-8-7908227*; Fax: *+46-8-105228*

E-mail*: rasmuson@ket.kth.se*.

Abstract

Butyl paraben crystals having a porous layer in between two solid non-porous layers have been produced by cooling crystallization in mixtures of ethanol and water. The outer layers are transparent and fully crystalline while the middle layer appears to be polycrystalline and is full of pores of various dimensions, down to below 0.1 μm diameters. The thickness of the porous layer reaches about 40 % of the whole crystal. The crystals contain one polymorph only and appear to be essentially fully crystalline. They are stable for more than a year when stored on the shelf at room temperature. When the crystals dissolve, the porous layer dissolves faster leaving the outer layers for a more slow dissolution. The sandwich crystals are easily cleaved through the middle layer parallel to (100) plane. This type of sandwich crystals may provide new useful properties to pharmaceutical solids, e.g. larger specific surface area, higher dissolution rates and improved compaction properties.

Keywords: sandwich crystals, butyl paraben, multiporous, cooling crystallization, ethanol, water, layer, LLPS, ternary diagram

Introduction

Crystallization is widely used for purification of compounds in the pharmaceutical industry, but can also be used to produce a solid material with properties more adapted to downstream processing and end-use. This property design can include tuning of crystal size and shape distributions, formation of agglomerates with advanced properties as in spherical crystallization[1], or formation of a particular polymorphic phase[2]. In some cases more complex particles are obtained on purpose or by accident, e.g. the layered mixed polymorph particles of sulphathiazole[3]. Because of the high specific surface areas[4], the microporous structure[5] found in zeolites[6], metal–organic frameworks[7] and organic polymer frameworks have excited interest for use in gas storage, molecular separation, and heterogeneous catalysis.. A porous structure is seldom found in small organic compound crystals, however, in the present work, we describe particles of butyl paraben composed by layers having distinctly different properties, where the middle layer is full of pores of various dimensions, from several μm to below 0.1 μm. Butyl paraben has been used for many years as a preservative in cosmetic and pharmaceutical products[8], and is generally considered to be safe. The compound is used for its antifungal properties[9, 10], and is said to stabilize formulations without the oxidation of active ingredients, thus increasing the shelf life.

There is only one polymorph [11, 12] reported for butyl paraben. However, the crystal structure is difficult to determine with high quality even at 77K because of the vibration of several carbon atoms in the hydrocarbon tail (Figure 1) of the molecule. Butyl paraben has a melting point[13] of 67.3 °C and is well soluble in ethanol[14] but very poorly soluble in water[15]. At higher concentrations butyl paraben induces liquid-liquid separation in ethanol-water mixtures[15, 16]. The ternary diagram of butyl paraben in ethanol and water has been determined from 1 °C to 50 °C in previous work[15], and in the present work sandwich type crystals have been produced by cooling crystallization in a liquid-liquid dispersion of butyl paraben-ethanol-water solution. The crystals have fairly distinct outer layers of translucent non-porous material enclosing an, opaque and porous layer in the middle, the properties of which have been investigated in this work.

Materials and method

Materials

Butyl paraben > 99.0% purity was purchased from Aldrich and was used without further purification. Ethanol of 99.7% purity from Solveco chemicals was purchased from VWR, and distilled water was used.

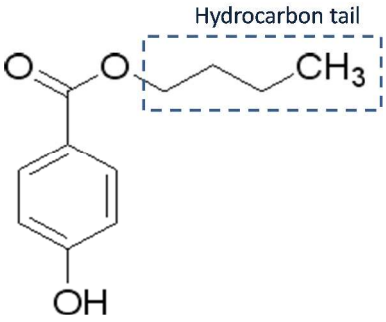

Figure 1. Molecular structure of butyl paraben

Methods

Experiments were performed in a 1 L jacketed glass cylindrical, un-baffled crystallizer, agitated by an impeller with a stirring rate of 200 rpm. The temperature in the crystallizer was controlled by a refrigerated circulator: Julabo FPW52-SP. About 500 ml solution with 29.9 weight % butyl paraben, with 45.6 weight % water and with 24.5 weight % ethanol was heated to 45.0 °C and equilibrated for 30 minutes, after which the solution was cooled down to 5.0 °C at the rate -0.1 °C per minute. The saturation temperature of the solution was approximately 20 °C. The cooling process is illustrated in the phase diagrams of Figure 2. ★ marks the composition of the starting solution inside region 2, in which the mixture at temperatures from 45 to 30 °C is a liquid-liquid dispersion[15] of a butyl paraben lean ethanol-water solution and a butyl paraben rich ethanol-water solution. Upon cooling, the mixture enters region 4 and becomes supersaturated with respect to butyl paraben. At further cooling the liquid-liquid dispersion eventually turns into a homogenous liquid phase in region 3.

The crystals obtained were examined by optical microscopy (Olympus SZX 12) and by SEM (Hitachi S-4800). From a bed of randomly displaced product crystals (below called "sandwich crystals) the IR Spectrum (PerkinElmer HATR) and the PXRD pattern (PANalytical X'Pert PRO) of the product crystals were determined. The different layers of the sandwich crystals were examined by Confocal Raman Microscopy, using a WITec alpha300 system (WITec GmbH, Germany) with a 532 nm laser for excitation, and an objective with 100× magnification and numerical aperture NA = 0.9. The optical parameters give a lateral resolution of 500 nm. A spot of about 0.2 μm^2 on each layer was examined. For each Raman spectrum, 10 spectra were collected, each recorded with an integration time of 0.5 s. The data was evaluated using the software program WITec project 2.06 (Ulm, Germany).

The thermal properties of the solid product where examined by a differential scanning calorimeter (TA Instruments, DSC 2920) calibrated against the melting properties of indium. Samples (2.0 to 3.0 mg) of butyl paraben crystals in standard sealed Al pan were heated by 5.0 °C per minute from 13.0 °C to 113.0 °C (the end point being approximately 50.0 °C above the melting temperature), then cooled down to 13 °C, and the cycle repeated two times for each sample.

Hot stage (Mettler FP 82) microscopy (Olympus BH-2) was performed on several product crystals. Sandwich crystals of butyl paraben were put on a glass slide, sealed by silicone oil, and then covered by a small coverslip. The hot stage was pre-heated to 50 °C after which the samples were heated by 0.5 °C per minute to 75.0 °C while taking pictures by a Hitachi HV-C20 camera connected to the microscope.

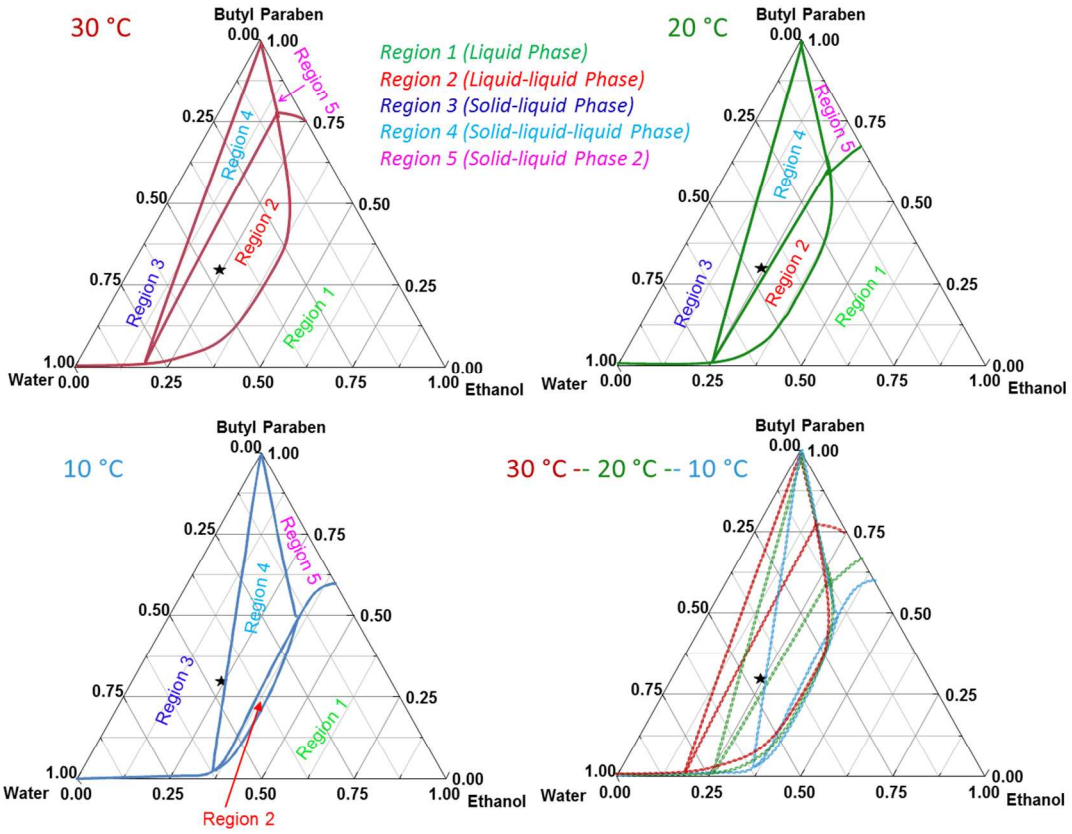

Figure 2. Cooling crystallization schedule of the solution '★' with certain concentration of butyl paraben, ethanol and water in the ternary phase diagrams[15] from 30 °C to 10 °C

Transformation of the sandwich crystals in a saturated solution at room temperature were observed on a watch glass under the microscope (Olympus SZX 12) using a camera (Olympus U-CMAD-2). Normal butyl paraben crystals were dissolved at room temperature in ethanol under agitation, assuring there was solid phase in the solution at equilibrium. The saturated solution was transferred onto the watch glass by a syringe equipped with a needle. The sandwich crystals were place in the solution and the transformation process was recorded every 30 seconds.

Single crystal X-ray diffraction data was collected in full sphere strategy. The crystal, either a normal crystal or a sandwich crystal, was mounted on an Oxford Diffraction Xcalibur CCD diffractometer with Mo Kα radiation (λ = 0.71073 Å). Unit cell indexing, face indexing and data reduction were performed using the CrysAlisPro program (Crysalis Sofware system Version

171.35.19). Gaussian adsorption correction was applied. The structure was solved by the direct method. Non-hydrogen atoms were located directly from difference Fourier maps. Final structure refinements were performed with the SHELX program by minimizing the sum of the squared deviation of F^2 using a full matrix technique [17, 18].

Results and discussion

Typical sandwich crystals are shown in Figure 3. Nearly all the crystals obtained have the characteristic three parallel layers denoted as a sandwich structure. In dry state, the sandwich crystals are stable and the three-layered-structure remains even after more than a year of open storage at room temperature.

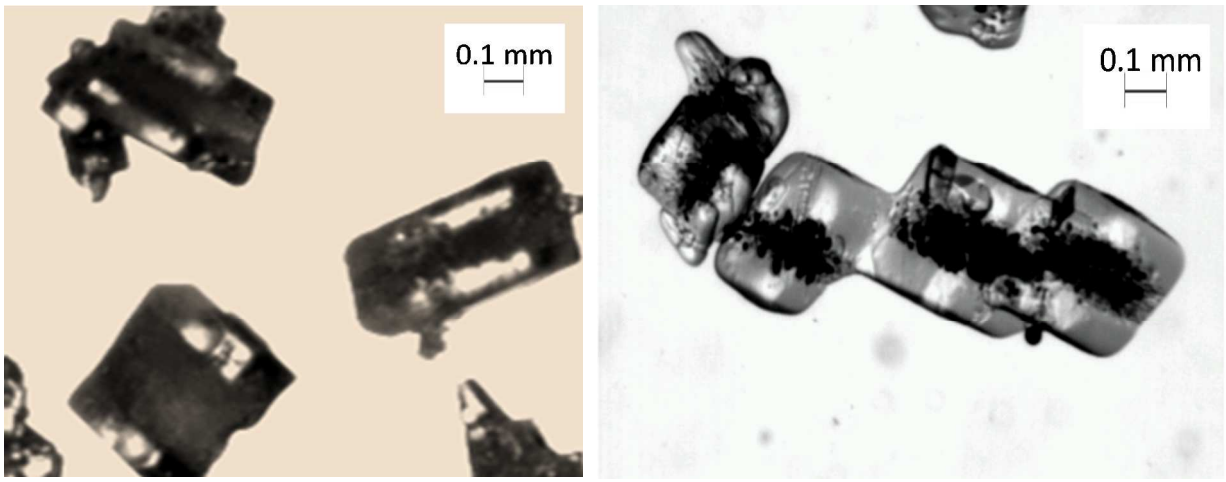

Figure 3. Microscopy images of sandwich crystals

Figure 4 compares PXRD patterns of the sandwich crystals and normal crystals (obtained from cooling crystallization in homogenous ethanol solution). The peaks at about 10.1 °, 12.4 °, 15.0 ° and 17.9 °, 20.4°, 21.5 ° and 28.3 ° are very much the same, while above 30 ° some differences can be noted. The sandwich crystals have more sharp peaks at about 34.8 and 53.0 than the normal crystals. For the ground normal and sandwich crystals there are two peaks at about 21.4 ° and 25.0 °, where the ground sandwich crystal shows only one peak, and for ground sandwich crystals, peaks above 30 ° are not very clear and distinguishing. Since, (i) nothing more than one polymorph has been found for butyl paraben, (ii) further results below does not reveal evidence of a solvate, and (iii) the peaks above 30 ° are not very clear and distinguishing, we claim no presence of more than one polymorphic form in the sandwich crystals. However, in PXRD

pattern for the ground sandwich crystals in Figure 4 the baseline is slightly convex which can be an indication of some amorphous content in the solid phase after grinding.

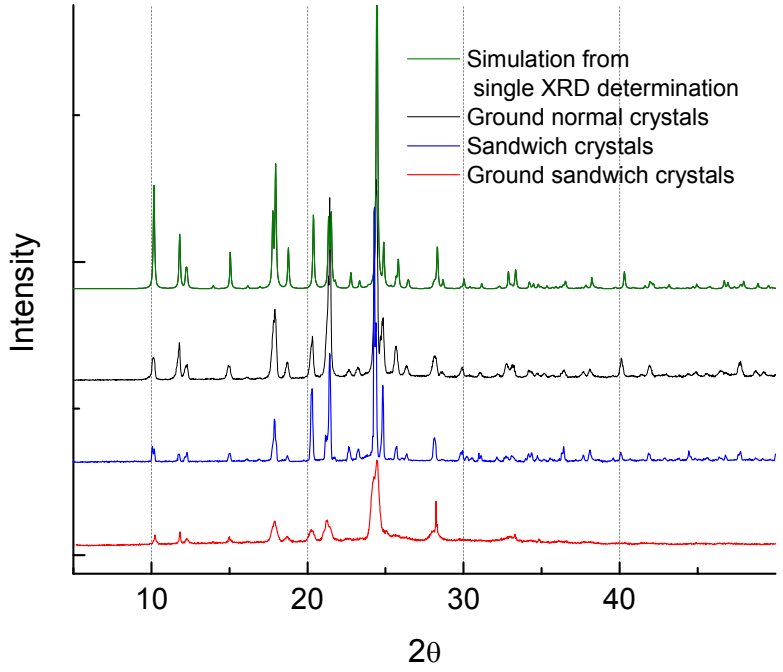

Figure 4. PXRD patterns of sandwich crystals not ground and well ground compared with the pattern of well ground normal crystals and simulated pattern from single XRD determination.

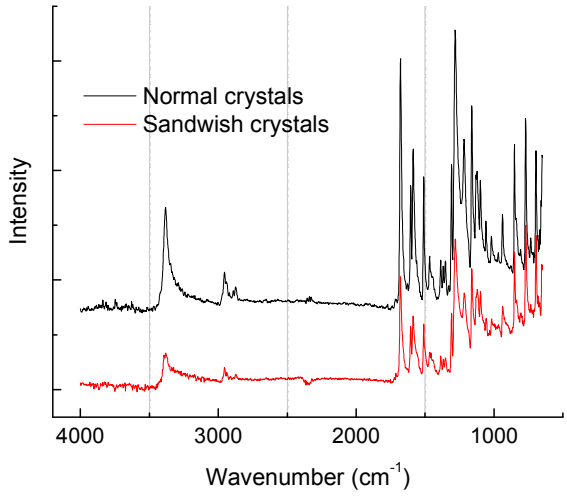

Figure 5. IR spectra of sandwich crystals and normal crystals

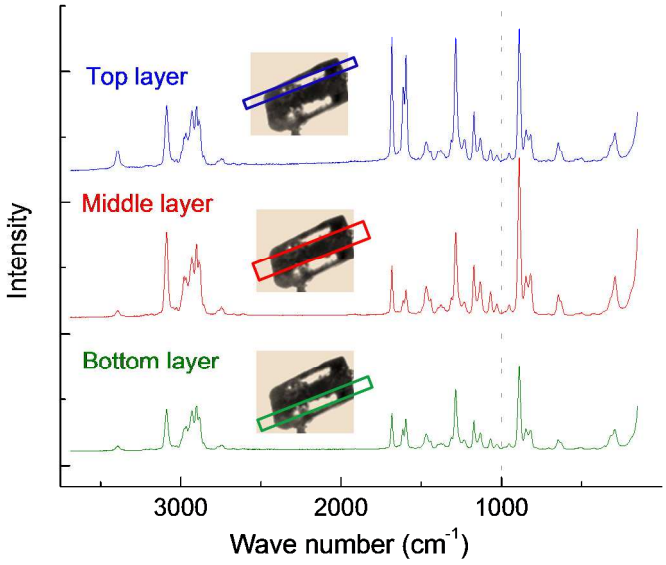

Figure 6. Confocal Raman spectra of the three layers

Figure 5 reveals that the IR spectra of the sandwich crystals and of normal butyl paraben crystals are almost identical except for a small difference at about 2400 cm^{-1} wavenumber (may be due to CO_2 from the atmosphere) and a small difference at about 1006 - 973 cm^{-1} wavenumber maybe

resulting from the C-C (carbon tail) vibrations. The full widths at half maximum height of the normal crystals are narrower than that of the sandwich crystals for most IR peaks in Figure 5, indicating disorder [19] inside the sandwich crystals compared with the normal crystals. The Confocal Raman spectra [20] of the three different layers of the sandwich crystals are essentially identical as shown in Figure 6. The strong similarities of PXRD patterns, Raman spectra and IR spectra reveal that the sandwich butyl paraben crystals and normal crystals are of the same polymorphic form. In addition, below we discuss the single crystal XRD (Figure 7 and Table 1) of the sandwich crystals which shows the same space group and highly identical unit cell parameters as reported in literature[21].

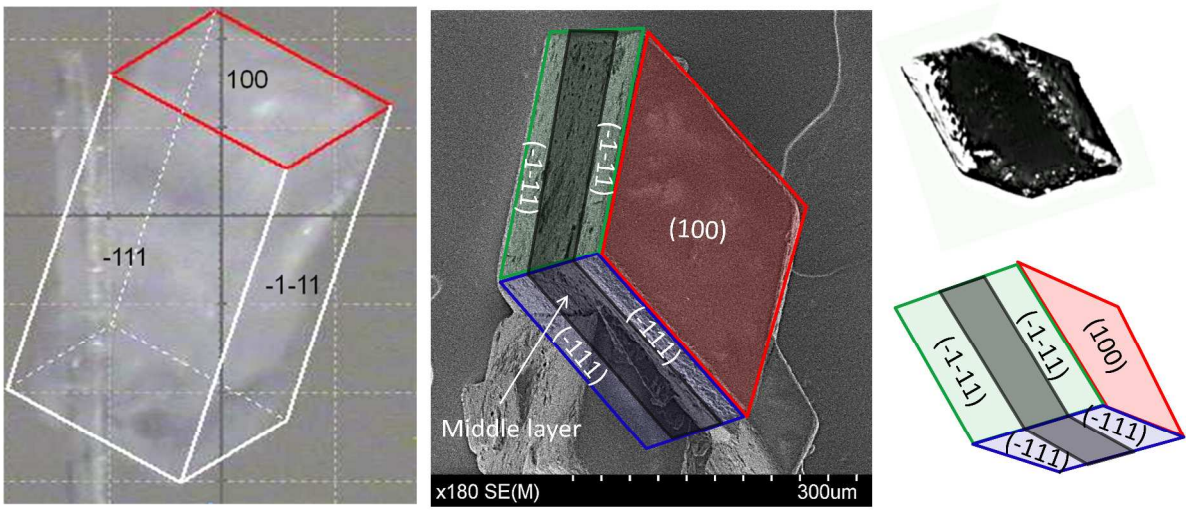

Figure 7. The morphology of the sandwich crystal.

Table 1. Crystallography of the sandwich crystal.

	Unit cell	Volume	Index Ratio	Separate	Overlapped
Perfect crystal*	20.081 Å, 8.179Å, 14.690 Å, 90.00 °,121.59 °, 90.00 °	2055.4 Å^3			
Sandwich crystal Twin 1	20.1177Å, 8.2320Å ,14.7466Å, 90.030 °, 121.405 °, 89.940 °	2084.4 Å^3	4179 (38.8%)	3210 (29.8%)	969 (9.0%)
Sandwich crystal Twin 2	20.1123Å, 8.2262Å, 14.7367Å, 89.957 °, 121.335 °, 90.074 °	2082.5 Å^3	3441 (31.9%)	2476 (23.0%)	965 (9.0%)
Sandwich crystal Twin 3	20.2286Å, 8.2325Å, 14.8749Å,	2102.8 Å^3	1003	879	124 (1.2%)

	89.960 º, 121.910º, 89.858 º		(9.3%)	(8.2%)	
Sandwich crystal Twin 4	19.7953Å, 8.1969Å, 14.6313Å, 89.953 º, 120.932 º, 89.803º	2036.4 Å^3	735 (6.8%)	607 (5.6%)	128 (1.2%)
Sandwich crystal Twin 5 - Sandwich crystal Twin n	2534 (23.5 %) unindexed spots, Index Ratio of each Sandwich crystal Twin < 735 (< 6.8%).				

*obtained by slow evaporation of butyl paraben-pure ethanol solution.

The sandwich crystal morphology is shown in Figure 7. The outer plane parallel to the middle layer can be indexed as the (100) face, and the other two main faces are indexed as (-111) and (-1-11), respectively. Most of the single crystal XRD reflections are quite round, except for some along *a**, showing irregular shape caused by the overlapping of different twin domains, which is further proved by using different twin domains to index the full Ewald sphere data. When two twin matrixes are used, 38.8% and 31.9% reflections can be indexed, respectively, covering in total 70.7 % of all reflections, Table 1. As shown in Figure 8a, these two matrixes are slightly tilted in *a** axis direction. When the third largest matrix is added to index the full sphere data another 9.3 % is accounted for (Table 1). This matrix is obviously deviating from the first two as shown in Figure 8b. When the fourth largest twin matrix is added, additional 6.8 % of reflections can be indexed (Figure 8c), with a much more serious deviation from the two dominating twin matrixes. The remaining 23.5 % of un-indexed reflections are due to lots of smaller crystal twin domains shown in Figure 8d. The index results indicate that the first and second biggest twin domains represents the outer layers, both well-ordered and with similar unit cell properties, but slightly misaligned along a*. However, the middle layer contains lots of small more randomly orientated crystals.

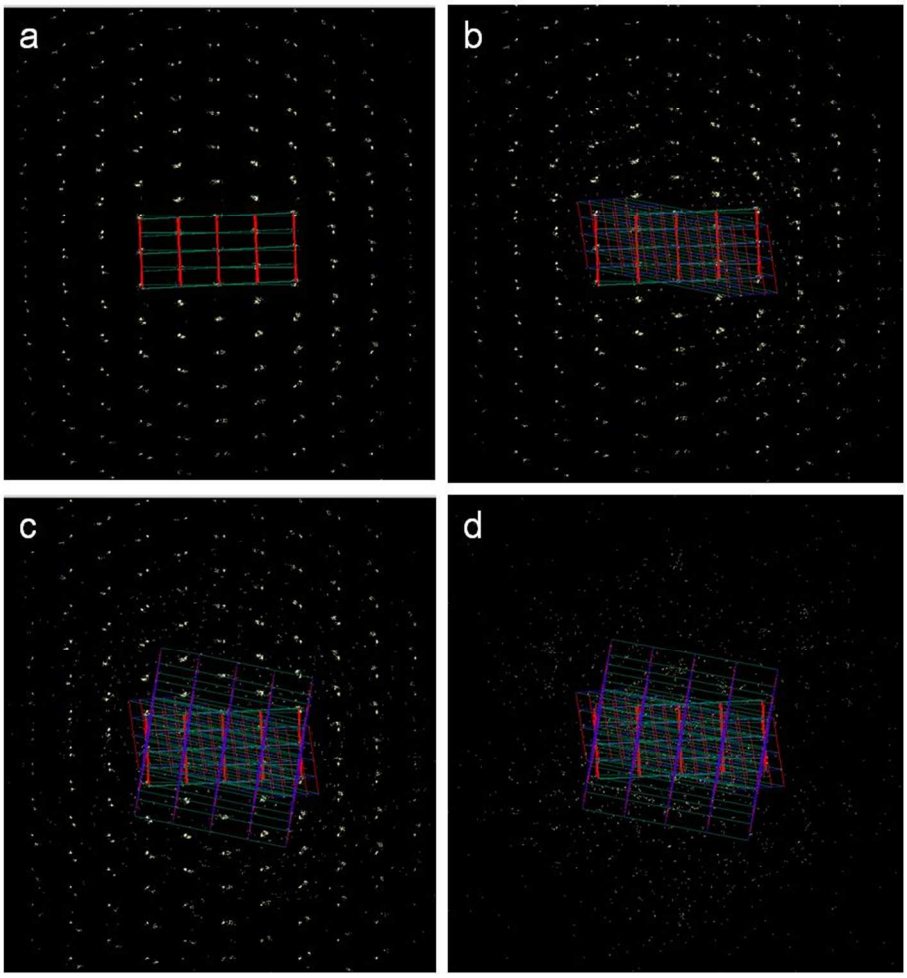

Figure 8. Twin matrix used to index the whole Ewald sphere data in reciprocal space for the sandwich crystal. a) The main two twin lattices; b) Three main twin lattices; c) Four twin lattices; d) The unindexed spots.

Figure 9 shows the crystal unit cell and molecular stacking in (100) plane, (-111) plane and (-1-11) plane. The (100) plane is perpendicular to the aliphatic hydrocarbon chain, the (-111) and plane (-1-11) are parallel to that chain. As shown in Table 1, compared to a perfect crystal, the crystal unit cell of the sandwich crystal outer layers is a bit larger, maybe resulting from the variability in the hydrocarbon chain stacking (some of the reflection spots in unwrap image show unregular shapes as shown in supporting material).

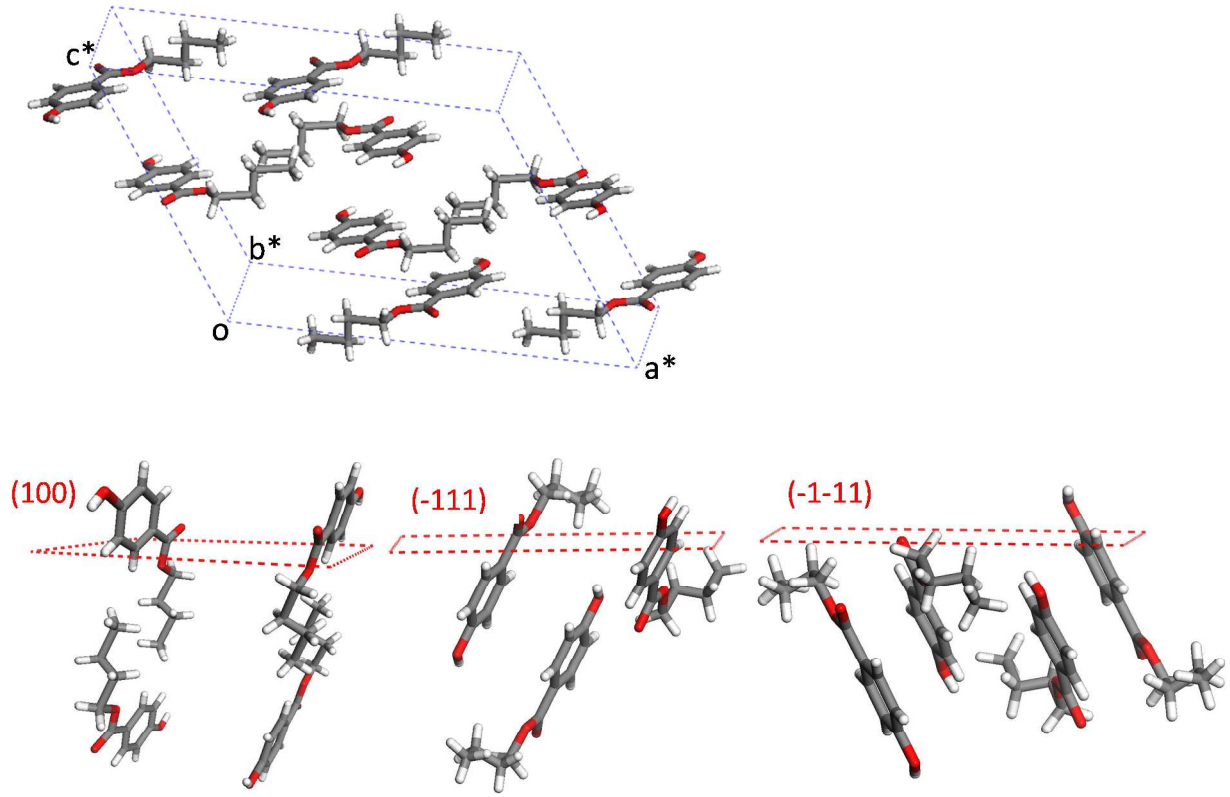

Figure 9. Unit cell of butyl paraben and the molecule stacking in (100) plane; (-111) plane; (-1-11) plane

Figure 10 shows SEM images of the sandwich crystals, the whole crystal or focused on the middle layer outside surface. Figure 10 (a), (b) and (c) show the three layers, and obviously the outer layers are smooth and flat, while the middle layer is irregular, rough and porous. Figure 10 (d) shows the porous structure of the middle layer and the sizes of the pores are in the order of 0.1 μm.

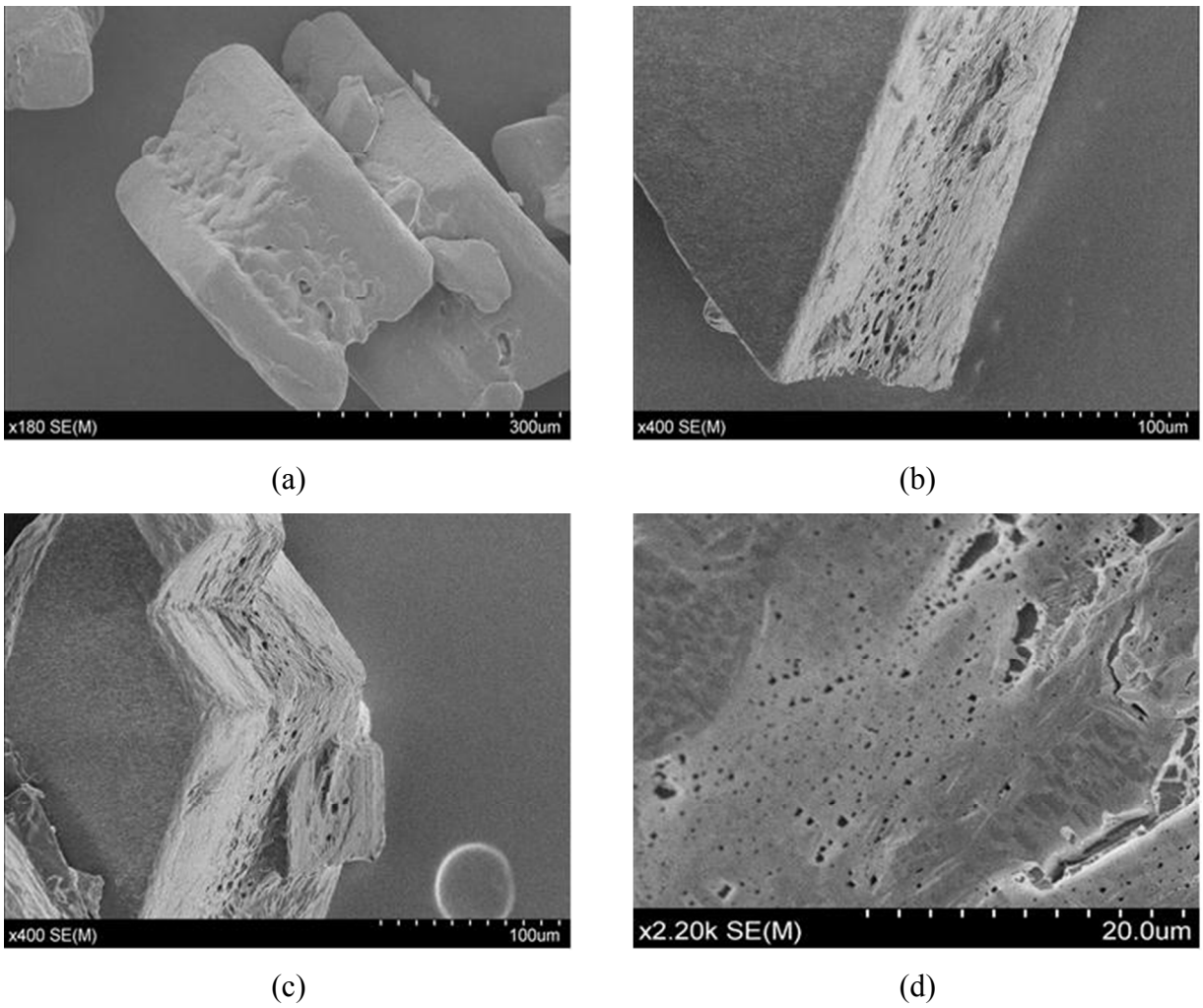

Figure 10. SEM images of the outside sandwich crystals

Also inside the crystal, the middle layer is porous, shown as sectional views in Figure 11. The pores appear to have a random distribution in direction and size, the latter ranging from several μm to below 0.1 μm in diameter as shown in Figure 12. The sandwich crystals are easily cleaved through the middle layer parallel to the (100) plane inside the middle layer. The porosity of the middle layer should lead to that these particles have an increased surface area for dissolution.

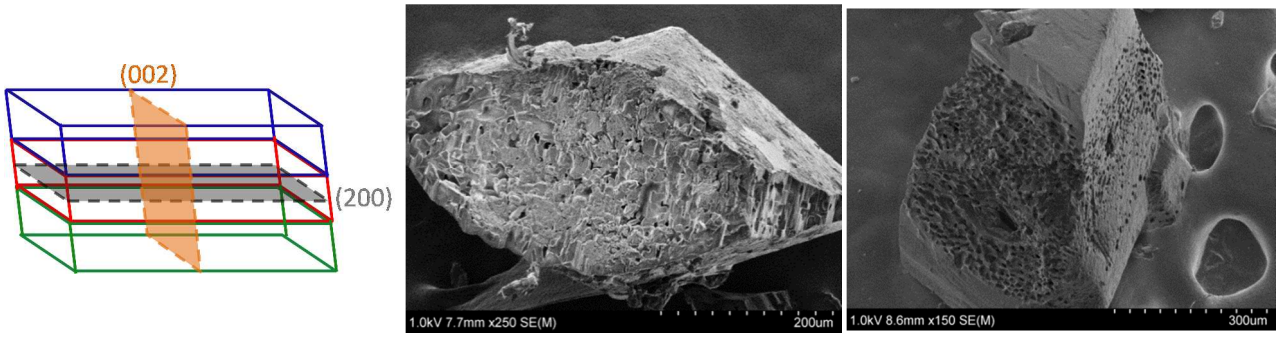

Sectional planes (200) (002)

Figure 11. SEM images of sectional planes (200) and (002)

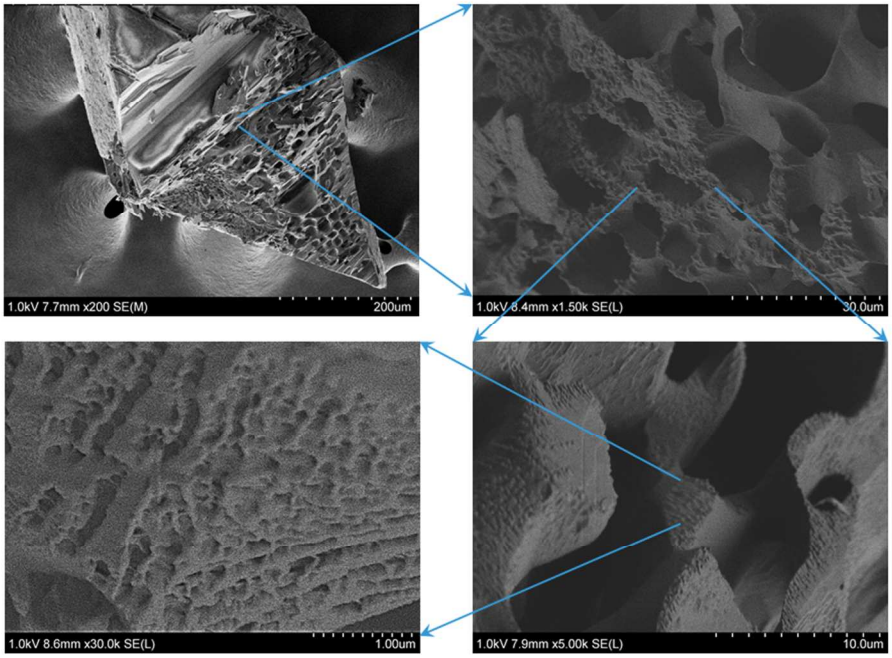

Figure 12. Examination of the porous structure inside the sandwich crystals. Pores with several μm to below 0.1 μm diameters.

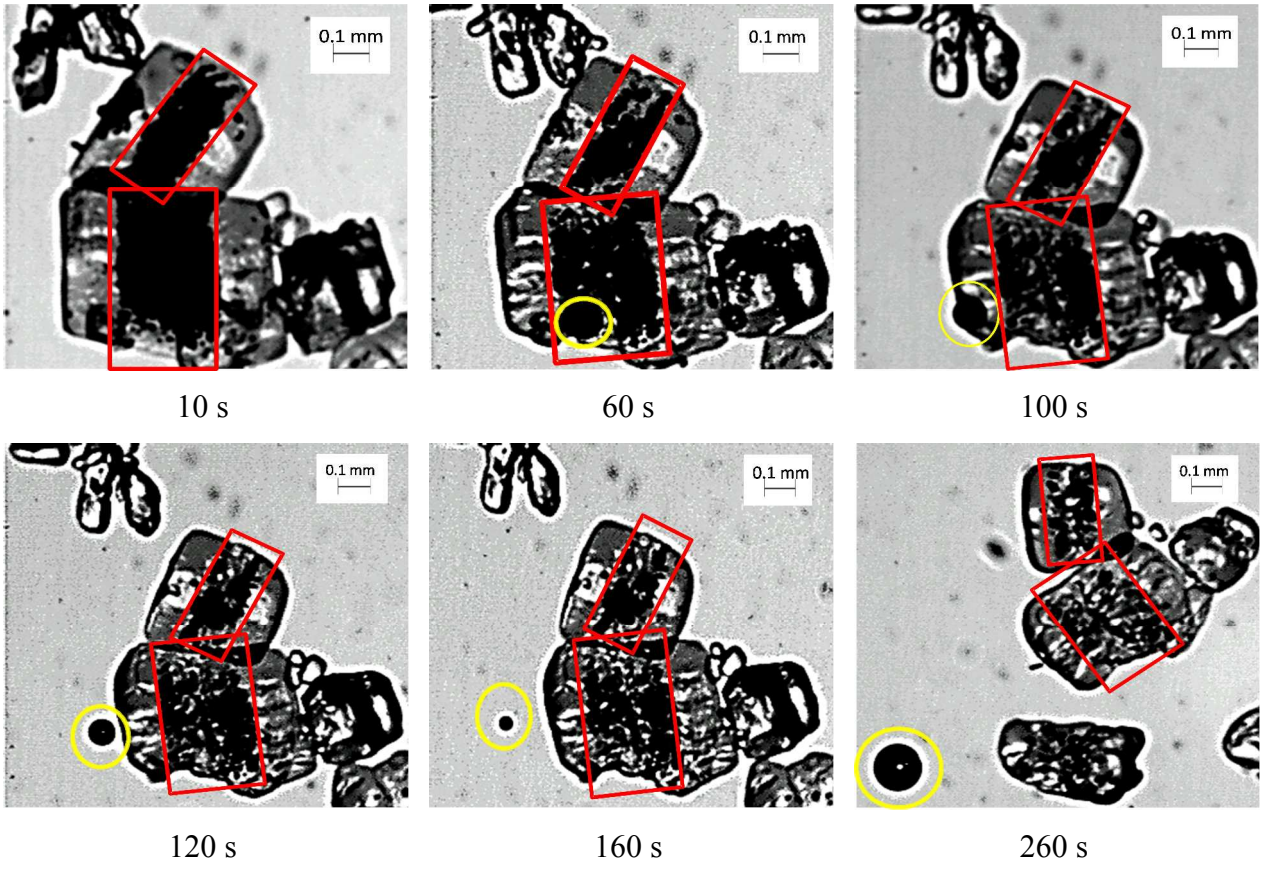

Figure 13. Transformation of sandwich crystals in saturated solution at room temperature. Red rectangles highlight the transforming middle layers and yellow circles highlight the air bulbs.

Figure 13 shows the transformation of sandwich crystals in a saturated solution at room temperature. The middle layer is originally black in the photographs revealing its opaque nature while the surrounding layers are more translucent. However, when the crystals in the saturated solution are maintained under the microscope, within a few minutes the middle layer becomes gradually more translucent as if the porosity or at least the entrapped air is gradually disappearing. As marked by yellow circles the images from 60 s to 160 s show one air bubble that is formed inside the middle layer during dissolution, and is released into the solution to finally disappearing. The image at 260 s shows another big air bubble appearing in the lower left corner. It appears as if the appearance of air bubbles can be used as an indicator of the transformation of the porous layer.

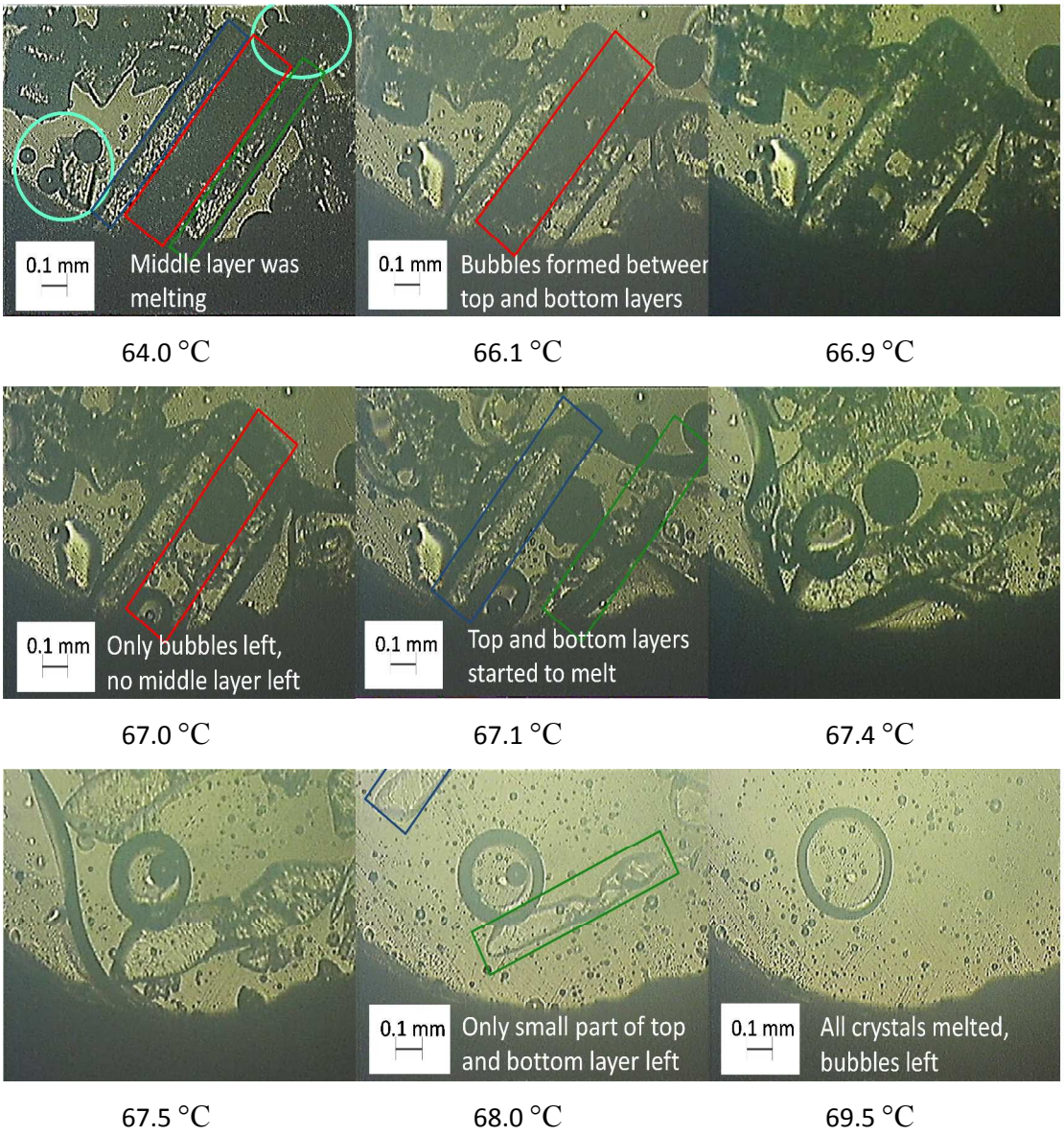

Figure 14. Hot stage microscope images of the melting process of the sandwich crystals. Top, middle and bottom layer are highlighted with blue, red and green color. Some small sandwich crystals with air bulbs are highlighted with light green color.

The melting process of sandwich crystals from 64.0 °C to 70.0 °C shown in Figure 14. Before 64.0 °C, no obvious change of the big sandwich crystal in the middle of the picture is observed but the middle layer of some small crystals (as highlighted by the light green circles) has melted, leaving some tiny crystals with air bubbles in the melt in the first image of Figure 14. The red

rectangle marks the porous middle section of the large sandwich crystal, while the blue and green rectangles mark the outer layers. At 66.1 °C, tiny bubbles have formed inside the middle layer of the larger sandwich crystal with the melting process. Above 66.1 °C, the middle layer quickly melts and fully disappears at 66.9 °C, while the outer layers remain unmelted with several bubbles in between. From 67.0 °C to 68.0 °C, two flat crystals originating from the two outer layers of the sandwich crystals begin to melt, and all solid phase has disappeared at about 69.5 °C. After that only bubbles of various sizes are left in the mixture of liquid butyl paraben and silicone oil. The hot stage microscopy images reveal that the middle layer has a slightly lower melting point than the material in the outer layers.

Figure 15 shows DSC curves for the sandwich crystals and for normal crystals. On the heating curve from the first cycle of the sandwich crystal, there is an endothermic broad peak before the appearance of the melting peak. In the repeated heating cycle of the same sample that small peak before melting peak has essentially disappeared. The small endothermic peak might indicate that the middle layer crystal lattice of the sandwich crystal is more disordered than that of the outer layer crystal and the normal crystals. In the second heating cycle, the peak value and the onset value of the melting peak is the same as for normal crystals. However, in the first heating cycle the onset value in particular but also the peak value determined for the sandwich crystals are about 1.0 °C lower than for normal crystals. The explanation can be that in the heating process from the first cycle, the porous material has a lower melting temperature, corresponding to reports in the literature that the melting point decreases with decreasing particle size [22-24]. However, since the previous melting should have destroyed all features related to the sandwich structure, it is surprising to find that the tiny peak has not disappeared entirely in the second heating cycle.

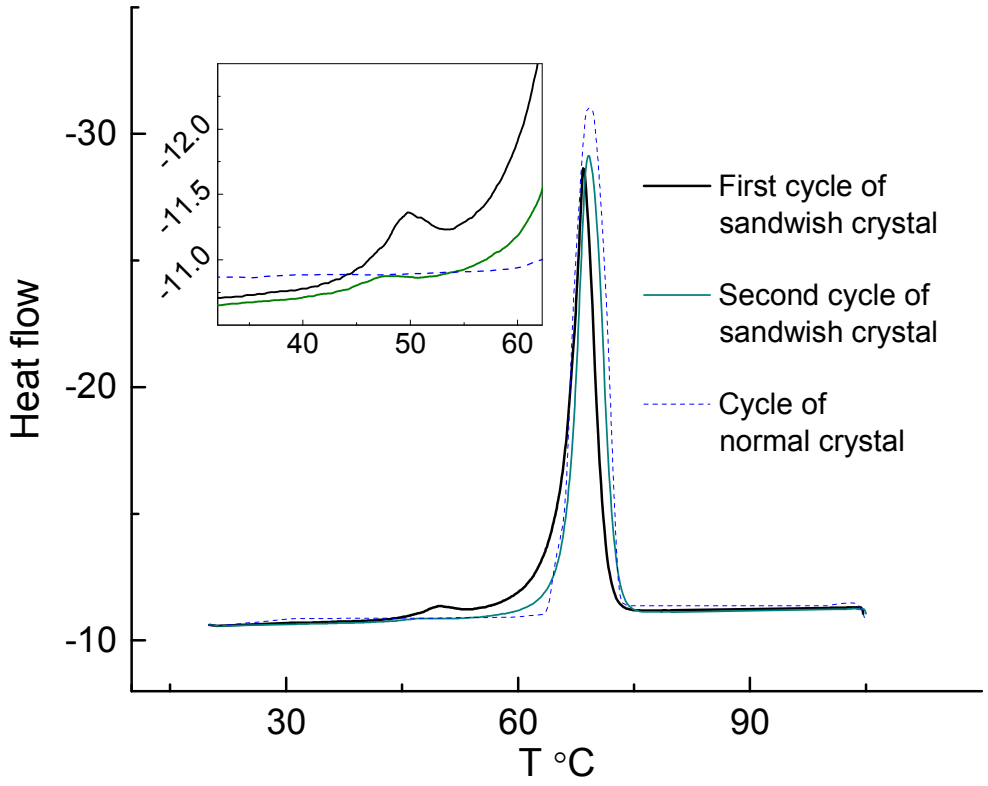

Figure 15. DSC curves of the sandwich crystals and normal crystals

By microscopy, the thicknesses of the different layers were measured, by observing randomly selected crystals lying on the glass slide with the layered structure perpendicular to the observation direction. The thicknesses of the whole crystal and of each layer were determined with the help of measuring tools in the software of the Olympic optical microscope, which had been calibrated by a stage micrometer previously. Figure 16 shows data for a total of 110 crystals, arranged in order of increasing overall crystal thicknesses from left to right in Figure 16a. The thicknesses of the middle layer range from 0.05 mm to 0.34 mm, while the thicknesses of the whole crystal range from 0.19 mm to 0.69 mm. The relative thicknesses of the middle layer to the total particle thicknesses range from about 20 % to about 60 %, having a value of about 40 % in majority. The middle layer thicknesses are proportional to the overall crystal thicknesses with the correlated line having a slope of 0.38 shown in Figure 16b. The ratio between the thicknesses of two outer layers to the thicknesses of the middle layer is similar to the ratio between the sum of index ratios of the crystal twin domains 1 and 2 to the remaining twin domains (Table 1). This

indicates that the middle layer is disordered and polycrystalline while the top and bottom layers are ordered single crystal structures. The thicknesses of two outer layer appear to be approximately equal (Figure 16c) while the thicknesses of the middle layer are not obviously correlated to the thicknesses of the top layer. This may suggest that the outer layers are growing simultaneously, which is asynchronous to the growth of the middle layer.

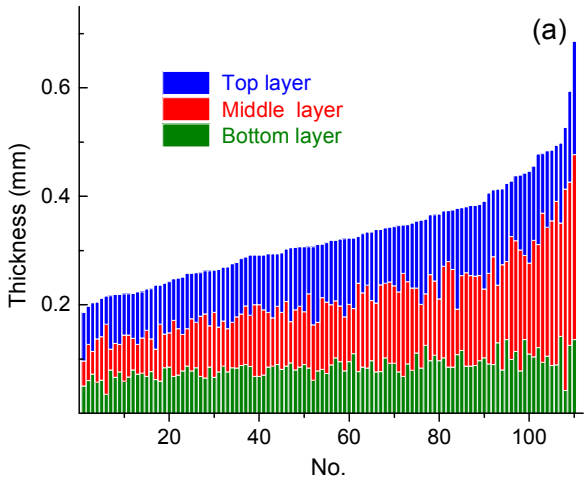

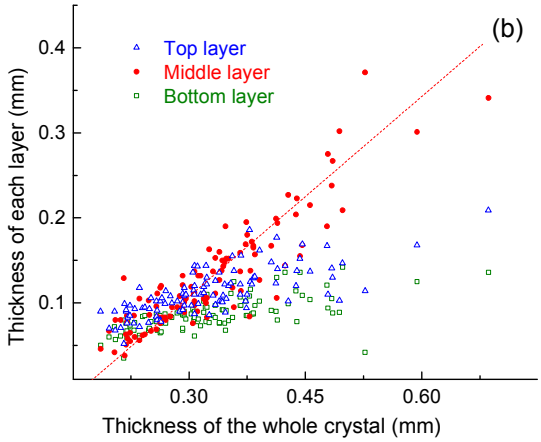

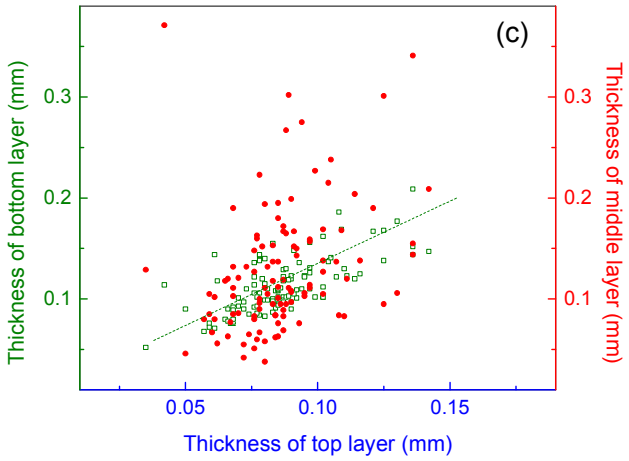

Figure 16. Thicknesses of the top (blue), middle (red) and bottom (green) layers of sandwich crystals. The top layer (blue) is selected as the outer layer having the larger thickness. The dashed lines in (b) and (c) are guiding line with least square fitting to the respective data.

Among thousands of sandwich crystals, several twin sandwich crystals are found, and one is shown in Figure 17. This twin sandwich crystal, is 'X'-shaped and so is the opaque middle layers. This indicates that the porous layer is formed early and the translucent layers are formed on the surface of the porous layer.

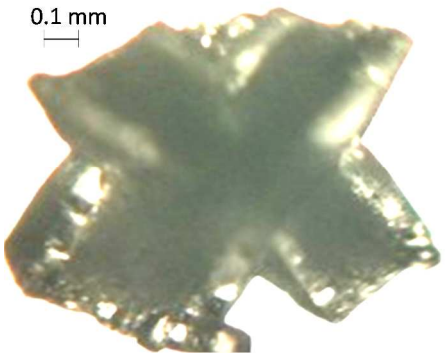

Figure 17. 'X' shaped twin sandwich crystal

Based on the analysis of the detailed properties, the relation between the thicknesses of the various layers (Figure 16) and the trajectory of conditions during the process, we propose the following steps in the formation of the sandwich crystals:

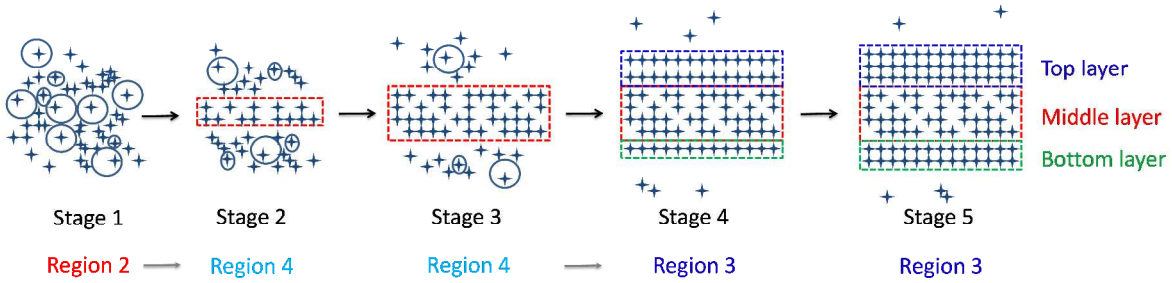

Figure 18 Proposed mechanism of sandwich crystal formation

The process starts in region 2 of the ternary phase diagram (Figure 2) at conditions where the liquid phase is a liquid-liquid dispersion, shown as stage 1 in Figure 18. In separate experiments, it has been found that this liquid-liquid dispersion at quiescent conditions (several hours) separates into two layers, where the top layer is lean in butyl paraben and the bottom layer has a fairly high concentration of butyl paraben. Upon agitation, the top layer becomes dispersed into the bottom layer. Accordingly, at approximately, 20 °C, solution enters into region 4 and supersaturation is generated in a liquid-liquid dispersion with a high concentration of droplets having a low concentration of butyl paraben and high concentration of water, and in a continuous phase with a high concentration of butyl paraben and low concentration of water. If this liquid-liquid dispersion is sampled and observed under the microscope, it can be established that crystals nucleate in the continuous phase. Accordingly, crystals initially nucleate and initially grow in a butyl paraben rich continuous phase however in close proximity to small water rich dispersed phase droplets. Since, the process is operated to primary nucleation, and the concentration of butyl paraben in the continuous phase is high, resulting in initially very fast nucleation and crystal growth rates. However, crystal growth becomes obstructed by the presence of the water rich dispersed phase droplets (stage 2 and 3 in Figure 18). Hence, without fully understanding the details, it is our hypothesis that the formation of the porous layer and its disorder, twinning[20] and polycrystallinity, are associated with this combination of rapid nucleation and obstructed crystal growth. As the cooling proceeds and the solution moves from

region 4 to region 3 (stage 4 in Figure 18), the liquid-liquid dispersion turns into a homogeneous liquid phase allowing for proper crystal growth and the formation of more homogenous, translucent and crystalline layers on top of the porous solid material.

The middle layer is porous and appears to be polycrystalline, while still having the same overall shape and crystal structure as that of the outer translucent layers. In our previous work[15], four different cooling crystallizations having a trajectory through the liquid-liquid phase separation region were performed. If we use the same labelling, the sandwich crystals were obtained in Exp 4 from a solution having approximately 30 % of butyl paraben, 45 % water and 25 % ethanol. If the solution contained approx. 53 % butyl paraben, 17 % water and nearly 30 % ethanol (Exp 2), or 44 % butyl paraben, 19 % water and almost 37% ethanol (Exp 3), the butyl paraben rich phase was still the continuous phase but the relative amount of dispersed phase was less, and only normal translucent crystals were obtained in the cooling crystallization. If the solution only contained nearly 12 % of butyl paraben, 58% water, and 30 % ethanol (Exp 5), the continuous phase is butyl paraben lean and the solid phase of product crystals was made up of small crystals heavily agglomerated into irregularly shaped particles. Accordingly, the appearance of the sandwich crystals is strongly related to the particular composition of the solution and the trajectory through the phase diagram upon cooling. At the conditions leading to sandwich crystals the relative amounts of the continuous and dispersed phases are approximately equal. According to this mechanism, we suspect that it should be possible to control the relative thickness of the porous layer by fine tuning the composition of the initial solution. In addition, we expect that the properties of the porous layer, e.g. the pore size distribution and the void volume, could be modulated by variations in the process design. These aspects are yet to be developed, but this type of sandwich crystals, may provide new useful properties to pharmaceutical solids, e.g. higher dissolution rates and improved compaction properties.

CONCLUSIONS

Crystals of butyl paraben with a sandwich structure have been produced by cooling crystallization in a solution that changes from a water-ethanol liquid-liquid dispersion into a homogeneous liquid phase. These sandwich crystals are characterized by an opaque and porous middle layer between two translucent nonporous layers. The porous middle layer has a lower

melting point and higher solubility, and appears to be polycrystalline or otherwise disordered. However, according to investigations by confocal Raman and IR spectroscopy, and PXRD the particles contain one polymorphic form only. The layers are essentially parallel to one another and to the dominating basal plane of the crystal. The thickness of the middle layer increases with increasing thickness of the whole crystal and on average amounts to about 40 %. The mechanisms by which these sandwich crystals are formed cannot be fully explained at this stage, but should relate to the fact that nucleation and growth start in a liquid-liquid dispersion solution with approximately equal amounts of the continuous and dispersed phases, and that the process ends in a homogeneous liquid phase.

ACKNOWLEDGMENT

Huayiu Yang gratefully acknowledges the scholarship from Chinese Scholarship Council and from the Industrial Association of Crystallization Research. The authors acknowledge the help at the Royal Institute of Technology of Fan Zhang with Raman analysis and of Bo Yin with SEM.

REFERENCE

1. B. Aziz, D. Gebauer and N. Hedin, *CrystEngComm*, 2011, 13, 4641-4645.
2. M. R. Thorson, S. Goyal, Y. Gong, G. G. Zhang and P. J. Kenis, *CrystEngComm*, 2012, 14, 2404-2412.
3. A. Munroe, D. Croker, Å. C. Rasmuson and B. Hodnett, *CrystEngComm*, 2011, 13, 831-834.
4. P. A. Wright, *Microporous framework solids*, Royal Society of Chemistry, 2008.
5. M. J. Bojdys, T. Hasell, N. Severin, K. E. Jelfs, J. P. Rabe and A. I. Cooper, *Chemical Communications*, 2012, 48, 11948-11950.
6. G. Majano, A. Restuccia, M. Santiago and J. Pérez-Ramírez, *CrystEngComm*, 2012, 14, 5985-5991.
7. S. Yang, L. Liu, J. Sun, K. M. Thomas, A. J. Davies, M. W. George, A. J. Blake, A. H. Hill, A. N. Fitch and C. C. Tang, *Journal of the American Chemical Society*, 2013, 135, 4954-4957.
8. C. Charnock and T. Finsrud, *Journal of Clinical Pharmacy and Therapeutics*, 2007, 32, 567-572.
9. I. T. Miettinen, T. Vartiainen and P. J. Martikainen, *Nature*, 1996, 381, 654.
10. M. Soni, S. Taylor, N. Greenberg and G. Burdock, *Food and Chemical Toxicology*, 2002, 40, 1335-1373.
11. F. Giordano, R. Bettini, C. Donini, A. Gazzaniga, M. Caira, G. Zhang and D. Grant, *J. Pharm. Sci.*, 1999, 88, 1210-1216.
12. H. Yang and Å. C. Rasmuson, *Cryst. Growth Des.*, 2013, 13, 4226-4238.
13. H. Yang, J. Thati and Å. C. Rasmuson, *J. Chem. Thermodyn.*, 2012, 48, 150-159.
14. H. Yang and Å. C. Rasmuson, *Journal of Chemical & Engineering Data*, 2010, 55, 5091-5093.
15. H. Yang and Å. C. Rasmuson, *Org. Process Res. Dev.*, 2012, 16, 1212-1224.

16. H. Yang and Å. C. Rasmuson, *Fluid Phase Equilibria*, 2014, 376, 69-75.
17. Sheldrick, *Acta Crystallogr. A*, 2008, 64, 112.
18. G. Sheldrick, 1997.
19. A. Ferrari, S. Rodil and J. Robertson, *Physical Review B*, 2003, 67, 155306.
20. A. Brillante, I. Bilotti, C. Albonetti, J. F. Moulin, P. Stoliar, F. Biscarini and D. M. de Leeuw, *Advanced Functional Materials*, 2007, 17, 3119-3127.
21. Y. Feng, D. J. W. Grant and C. C. Sun, *J. Pharm. Sci.*, 2007, 96, 3324-3333.
22. C. Wronski, *British Journal of Applied Physics*, 1967, 18, 1731.
23. D. Pan, L.-M. Liu, B. Slater, A. Michaelides and E. Wang, *ACS nano*, 2011, 5, 4562-4569.
24. M. Schmidt, R. Kusche, B. Von Issendorff and H. Haberland, *Nature*, 1998, 393, 238-240.

A table of content entry

Sandwich Crystals of Butyl Paraben

Huaiyu Yang, Hong Chen, Åke C Rasmuson

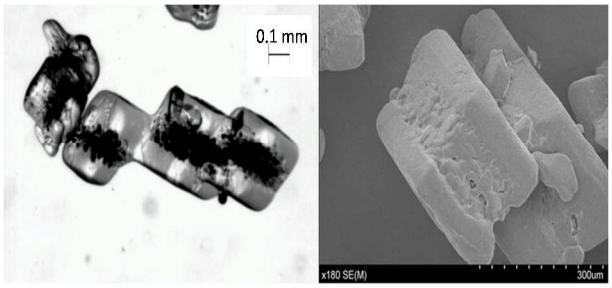

Sandwich Crystals: one polymorph. Opaque Middle Layer: 0.1 μm scale size pores. Parallel Outer Layer: translucent crystalline layers.